metals

MDPI

Article

Comparative Morphological and Crystallographic Analysis of Electrochemically- and Chemically-Produced Silver Powder Particles

Ljiljana Avramović [1], Miroslav M. Pavlović [2], Vesna M. Maksimović [3], Marina Vuković [4], Jasmina S. Stevanović [2], Mile Bugarin [1] and Nebojša D. Nikolić [2,*]

1 Mining and Metallurgy Institute-Department for Experimental Testing of Precious Metals, Zeleni bulevar 35, 19 210 Bor, Serbia; ljiljana.avramovic@irmbor.co.rs (L.A.); mile.bugarin@irmbor.co.rs (M.B.)
2 ICTM-Department of Electrochemistry, University of Belgrade, Njegoševa 12, 11 000 Belgrade, Serbia; mpavlovic@tmf.bg.ac.rs (M.M.P.); jaca@tmf.bg.ac.rs (J.S.S.)
3 Vinča Institute of Nuclear Sciences-Department of Materials Science, University of Belgrade, 11 000 Belgrade, Serbia; vesnam@vin.bg.ac.rs
4 Institute for Multidisciplinary Research, University of Belgrade, Kneza Višeslava 1a, 11 000 Belgrade, Serbia; marina.vukovic@imsi.bg.ac.rs
* Correspondence: nnikolic@ihtm.bg.ac.rs; Tel.: +381-11-337-0389

Academic Editor: Jürgen Eckert
Received: 27 March 2017; Accepted: 28 April 2017; Published: 5 May 2017

Abstract: Silver powders chemically synthesized by reduction with hydrazine and those produced by electrolysis from the basic (nitrate) and complex (ammonium) electrolytes were examined by X-ray diffraction (XRD) and scanning electron microscopic (SEM) analysis of the produced particles. Morphologies of the obtained particles were very different at the macro level. The needle-like dendrites, as well as the mixture of irregular and regular crystals, were formed from the nitrate electrolyte, while the highly-branched pine-like dendrites with clearly noticeable spherical grains were formed from the ammonium electrolyte. The agglomerates of spherical grains were formed by reduction with hydrazine. In the particles obtained from the nitrate electrolyte, Ag crystallites were strongly oriented in the (111) plane. Although morphologies of Ag particles were very different at the macro level, the similarity at the micro level was observed between chemically-synthesized particles and those obtained by electrolysis from the ammonium electrolyte. Both types of particles were constructed from the spherical grains. This similarity at the micro level was accompanied by the similar XRD patterns, which were very close to the Ag standard with a random orientation of Ag crystallites. For the first time, morphologies of powder particles were correlated with their crystal structure.

Keywords: silver; powder particles; chemical synthesis; electrolysis; scanning electron microscope (SEM); X-ray diffraction (XRD) analysis

1. Introduction

Metal powders attract an attention both academic and technological communities owing to their wide application in almost all branches of industry. The main techniques for production of metal powders are: atomization processes, melt spinning, rotating electrode process (REP), mechanical and chemical processes [1,2]. Metal powders are characterized by their morphology and size of the formed particles. The shape and size of particles strongly depend on a method used for their preparation.

The processes of electrolysis are widely used in production of metal powders, and about 60 metals can be successfully produced in the powder form by electrolytic procedure [3]. Formation of powders by electrolysis is an economical processing method with a low capital investment and operational cost.

Powders produced by electrolysis are of high purity with the possibility to be easily pressed and sintered and contain low oxygen content [4]. Advantages of metal powders production by electrolysis in relation to the other methods are: fast, simple, one-step, environmentally friendly, avoiding the use of vacuum systems or high temperatures processes and easier control of shape and size of the particles [5]. The electrolitically produced particles belong to the group of disperse (or irregular) morphological forms, that spontaneously fall down from the electrode surface during electrolysis, or are removed by tapping or by some similar techniques. The shape of powder particles depends on both the conditions of electrolysis, such as the current density or overpotential, the type and composition of electrolyte, temperature, the type of working electrode, regime of electrolysis, etc., and the nature of metals [6]. Although powder particles are the most often dendritic shape, they can also be in the form of flakes, fibrous, spongy, wires at sub-micrometer or nanometer scale, cauliflower-like, as well as in the many other irregular forms [4–16]. Various forms of dendrites are formed by electrolysis, and the shape of dendritic particles is primarily determined by the type of metals [4,6,9,11–14]. Hydrogen evolution as the second reaction during electrodeposition of metals can also make the strong effect on morphology of powder particles [16,17].

All metals that can be produced electrolytically from aqueous solutions can also be obtained using chemical methods, i.e., without an external current source [6,18]. The most important chemical processes for production of metal powders are hydrometallurgical method and electroless deposition. In hydrometallurgical method, the reduction of metal ions is achieved by hydrogen under pressure and at elevated temperatures, while the electroless deposition involves procedures a galvanic displacement (cementation or immersion) and an autocatalytic deposition. The galvanic displacement deposition is a heterogeneous process in which the noble metal is deposited at the surface of an active metal. The consequence is that the less noble (or active) metal is oxidized or dissolved in the appropriate solution. As a result, the ions of a more noble metal present in the solution are reduced leading to the deposition of the more noble metal [6]. The autocatalytic deposition proceeds only on the catalytically active surfaces. Initiation of the autocatalytic deposition is achieved by a proper choice of catalysts, reducing agents and stable solutions containing metal ions aimed to be reduced. The character of the reactions during the autocatalytic deposition and morphology of the deposit is significantly influenced by the catalytic activity of the metal particles formed in the reaction between metal ions and appropriate reducing agent.

The shape of chemically synthesized powder particles depends on method used for their synthesis, the nature of metals, the type of the solutions, temperature, pH, complexing and buffering agents, the type and concentration of reducing agent, stabilizers, the type of substrate, etc. [6,18–21]. It is necessary to note that most parameters affecting morphology of particles are the same for both electrochemical and chemical processes. This can cause the certain similarities in morphologies of particles obtained by the electrochemical and chemical processes.

Various silver particles are formed by above mentioned methods for powder production [6,19–25]. The interest for investigation of silver structures lies in their unique electrical, chemical, and optical characteristics. However, although numerous mechanisms of formation of Ag crystals are considered, there is no data correlating morphology of particles with their crystallographic structure. For that reason, the aim of this study was to establish it at the semi quantitative level. For those purposes, Ag particles of various shapes were produced via electrochemical and chemical routes, and characterized by the technique of scanning electron microscopy (SEM). The two types of electrolytes were used for production of Ag powders by electrolysis: the basic (nitrate) and complex (ammonium) ones. For chemical synthesis of Ag powder, hydrazine is used as reducing agent. Considering the fact that the X-ray diffraction (XRD) analysis is useful tool for structural analysis [26], this technique was used for a determination of preferred orientation of the produced particles.

2. Materials and Methods

2.1. Electrochemical Experiments

Silver particles were produced by a galvanostatic regime of electrolysis in an open cell at the room temperature using the following electrolytes:

(a) 0.10 M $AgNO_3$ in 2.0 M $NaNO_3$ (the nitrate electrolyte), and
(b) 0.10 M $AgNO_3$ in 0.50 M $(NH_4)_2SO_4$ with the addition of NH_3 to dissolve the silver sulfate precipitate (the ammonium electrolyte).

The polarization curves were recorded potentiostatically using an Ag wire for both the working and reference electrodes. The counter electrode was of Ag foil. The tip of the Ag reference electrode was situated at a distance of 2 mm from the surface of the Ag working electrode.

Doubly-distilled water and analytical grade chemicals were used for preparation of the electrolytes for the electrodeposition of silver. In the dependence of type of the electrolyte, Ag was electrodeposited at current densities of 14.4 mA cm^{-2} (the nitrate electrolyte), and 13.05 mA cm^{-2} (the ammonium electrolyte). These current densities were 1.5 times larger than the corresponding limiting diffusion current densities. For production of powder particles, platinum wire of a length 4.0 cm and a diameter 0.8 mm was used as the working electrode. The overall surface area of such a cylindrical Pt electrode was 1.0048 cm^2. The counter electrode was silver foil, having an overall surface area of 144 cm^2, situated close to the cell wall, while the working electrode was situated in the middle of the cell. For the both electrolytes, the particles were removed from the Pt working electrode every 10 min. After removal of the particles from the electrode surface, the particles were rinsed with the distilled water to remove traces of the electrolytes and dried in a tube furnace under a controlled nitrogen atmosphere at 110–120 °C for 16 h. The particles prepared in this way were further characterized by various techniques (see Section 2.3).

2.2. Chemical Synthesis

Ag powder was synthesized with hydrazine as a reducing agent in the following manner: white silver chloride precipitate was obtained by addition of hydrochloric acid to a silver nitrate solution. After filtration of the obtained precipitate, the same is rinsed with 1% HCl. In the next step, the silver chloride precipitate is dissolved in the excess of ammonium hydroxide and soluble ammonium complex of silver is obtained. Silver is reduced from this complex by a gradual addition of hydrazine as reducing agent with vigorous stirring. This reaction is exothermic one. The obtained Ag powder is filtered, rinsed with distilled water, and dried in a tube furnace under controlled nitrogen atmosphere at a temperature of 110–120 °C for 16 h. The chemically-synthesized particles were characterized in the same way as those obtained by the electrolytic processes.

The mechanism of formation of Ag particles with hydrazine as a reducing agent can be presented as follows:

Silver chloride is precipitated by addition of hydrochloric acid to silver nitrate solution according to:

$$AgNO_3 + HCl \rightarrow AgCl\downarrow + HNO_3.$$

Then, silver chloride precipitate dissolves itself in excess of NH_4OH according to reaction:

$$AgCl + 2NH_4OH \rightarrow [Ag(NH_3)_2]Cl + 2H_2O$$

and, finally, silver in the form of powder is formed by reduction with hydrazine according to:

$$[Ag(NH_3)_2]Cl + N_2H_4 \times H_2O \rightarrow NH_4Cl + NH_2OH + N_2 + 2.5\ H_2 + Ag.$$

2.3. Characterization

Morphologies of silver powder particles were characterized using a TESCAN Digital Microscopy scanning electron microscope (SEM, model VEGA3, Brno, Czech Republic).

The XRD (X-ray diffraction) analysis of the obtained powders was performed by the Rigaku Ultima IV diffractometer (Rigaku Co. Ltd., Tokyo, Japan), with CuKα radiation used for crystal structure examination, and four reflections were monitored for 2θ values ranging from 25° to 80°. For the evaluation of the preferred orientation, the "texture coefficient", *TC*(*hkl*) and the "relative texture coefficient", *RTC*(*hkl*) were calculated from the XRD data using the following procedure: for each reflection plane (*hkl*) monitored, the following ratio (in percentage) was calculated according to Equation (1) [27]:

$$R(hkl) = \frac{I(hkl)}{\sum_{i}^{4} I(h_i k_i l_i)} \times 100 \quad (1)$$

where $I(hkl)$ is the intensity of the (*hkl*) reflection, in cps, and $\sum_{i}^{4} I(h_i k_i l_i)$ is the sum of all intensities of the monitored reflections, in cps, for the powder particles under consideration.

The "texture coefficient", *TC*(*hkl*), for the reflection (*hkl*) is defined by Equation (2):

$$TC(hkl) = \frac{R(hkl)}{R_s(hkl)} \quad (2)$$

where $R_s(hkl)$ is defined in the same way as given by Equation (1), but is related to the Ag standard (4-0783).

Although the texture coefficient, *TC*(*hkl*), of a given reflection gives accurate quantitative information about the absolute intensity of the reflection, the intensity of the reflection relative to that of the other reflections also yields valuable information. Thus, the "relative texture coefficient", *RTC*(*hkl*) is defined by Equation (3):

$$RTC(hkl) = \frac{TC(hkl)}{\sum_{i}^{4} TC(h_i k_i l_i)} \times 100 \quad (3)$$

The *RTC*(*hkl*) coefficient expresses the intensity of a given orientation (*hkl*) relative to the standard (included in the *TC* values).

For a determination of the specific surface area of powders, MASTERSIZER 2000 (MALVERN Instruments Ltd., Malvern, Worcestershire, UK) was used. The values of the specific surface area (SSA) were obtained using the Malvern software which controls the apparatus operation and processes the obtained data.

3. Results

3.1. Electrochemical Production of Silver Particles: Polarization, Morphological, and Crystallographic Analysis

The polarization curves for electrodeposition of silver from 0.10 M $AgNO_3$ in 2.0 M $NaNO_3$ (the nitrate electrolyte) and 0.10 M $AgNO_3$ in 0.50 M $(NH_4)_2SO_4$ with the addition of NH_3 to dissolve silver sulfate precipitate (the ammonium electrolyte) are shown in Figure 1.

Unlike of the ammonium electrolyte showing the well-defined plateau of the limiting diffusion current density (the range of overpotentials corresponding to this plateau is between 250 and 700 mV), for the nitrate electrolyte this plateau is relatively short with the slope relative to the overpotential axis (70–110 mV). Irrespective of the type of used electrolytes, formation of dendrites as the most often shape of powder particles occurs in the diffusion controlled electrodeposition, i.e., at current

densities and overpotentials corresponding to plateaus of the limiting diffusion current density and at the higher ones [6].

Figures 2 and 3 shows silver powder particles obtained from the nitrate (Figure 2) and the ammonium (Figure 3) electrolytes. The shown powder particles are obtained by removal of disperse silver deposits formed by the galvanostatic regime of electrolysis at current densities which corresponded to 1.5 times larger values than the limiting diffusion current densities, i.e., at 14.4 mA cm^{-2} (the nitrate electrolyte; Figure 2) and at 13.05 mA cm^{-2} (the ammonium electrolyte; Figure 3). Similar to polarization curves, the strong difference is observed in morphology of powder particles obtained from these two electrolytes. The typical morphological forms electrodeposited from the nitrate electrolyte are: regular crystals with the well-defined crystal planes, irregular crystals, and the 2D (two-dimensional) needle-like dendrites (Figure 2). The specific surface area of the Ag powder obtained from the nitrate electrolyte (SSA_{NIT}) was 0.0329 $m^2\ g^{-1}$.

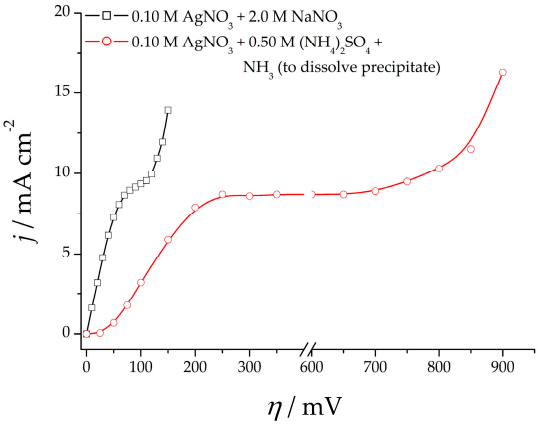

Figure 1. The polarization curves for silver electrodeposition from 0.10 M $AgNO_3$ in 2.0 M $NaNO_3$ (the nitrate electrolyte) and from 0.10 M $AgNO_3$ in 0.50 M $(NH_4)_2SO_4$ with the addition of NH_3 to dissolve silver sulfate precipitate (the ammonium electrolyte).

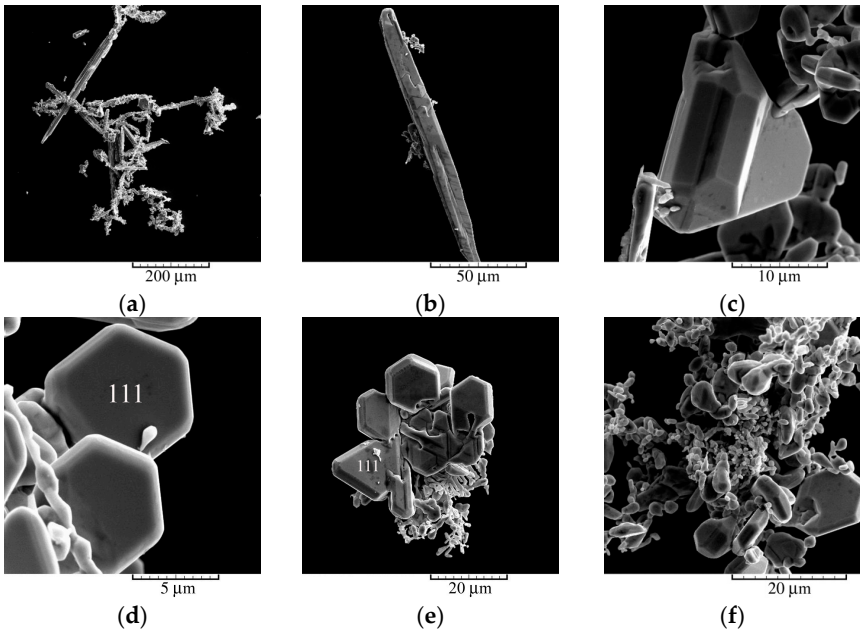

Figure 2. Ag powder particles obtained by electrodeposition from 0.10 M $AgNO_3$ in 2.0 M $NaNO_3$ at a current density of 14.4 mA cm^{-2}: (**a**) collection of the obtained particles; (**b**) the needle-like dendrite; (**c**–**e**) the typical regular crystals, and (**f**) collection of mostly irregular crystals.

The completely different morphologies of the particles were obtained with the use of the ammonium electrolyte (Figure 3). The highly-branched 3D (three-dimensional) pine-like dendrites without clearly defined crystal planes are formed by electrolysis from the ammonium electrolyte. It is interesting to note that the branches of dendrites (Figure 3a) were mutually parallel and oriented at an approximate angle of about 60° in relation to stalk or trunk indicating the existence of the growth of silver crystals along a preferential direction. The specific surface area of the powder obtained from the ammonium electrolyte (SSA_{AM}) was 0.0433 $m^2\,g^{-1}$, and it was larger than that obtained from the nitrate electrolyte.

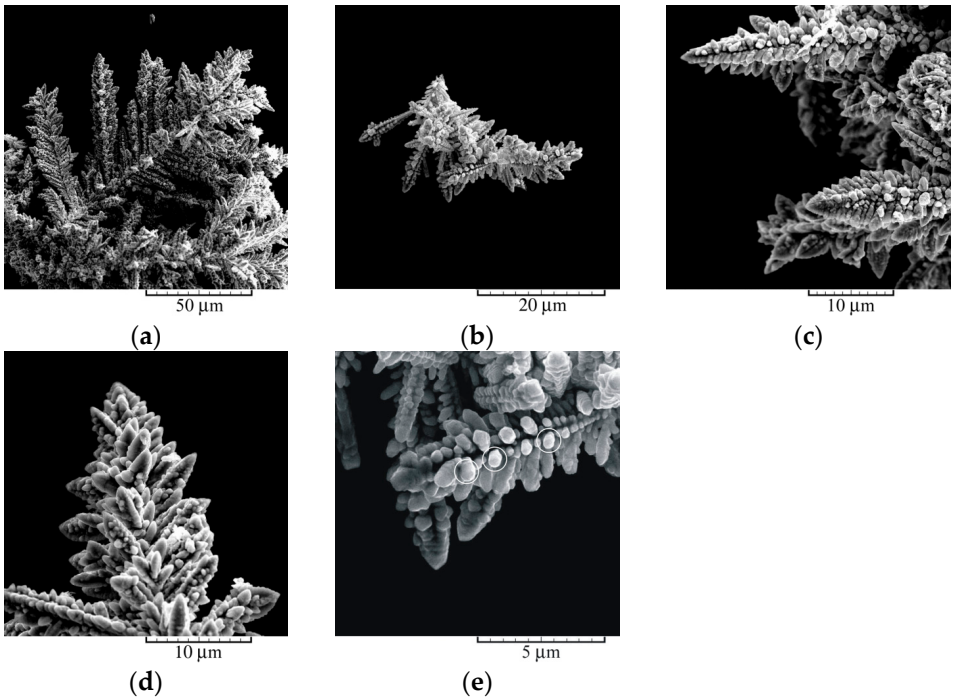

Figure 3. Ag powder particles obtained by electrodeposition from 0.10 M $AgNO_3$ in 0.50 M $(NH_4)_2SO_4$ with the addition of NH_3 to dissolve the silver sulfate precipitate at a current density of 13.05 mA cm^{-2}: (**a**,**b**) top view; and (**c**–**e**) the details of the particles shown under (**a**,**b**).

The XRD (X-ray diffraction) patterns of the particles shown in Figures 2 and 3 together with Ag standard (4-0783) are shown in Figure 4. The XRD patterns for the both types of particles show peaks with 2θ values at 38.1°, 44.3°, 64.4°, and 77.5°, which correspond to the (111), (200), (220), and (311) crystal planes, respectively. The appearance of the peaks at these angles confirms face centered cubic (FCC) structure of silver. Although the Ag crystallites were dominantly oriented in the (111) plane in the both types of powder particles, it is necessary to note that the ratio of crystallites oriented in the (200), (220), and (311) planes was larger in the particles obtained from the ammonium electrolyte than in those obtained from the nitrate electrolyte. The ratios of peak intensities (111)/(200), (111)/(220), and (111)/(311) for the Ag particles obtained from the both electrolytes, as well as for the Ag standard, are given in Table 1.

Table 1. Ratios of the intensities of the diffraction peaks for the analyzed powders and for the Ag standard.

The Type of Powder Particles	Ratio of Intensities		
	(111)/(200)	(111)/(220)	(111)/(311)
The nitrate electrolyte	4.2	9.3	9.9
The ammonium electrolyte	2.5	4.8	4.9
Reduction with hydrazine	3.0	4.7	4.8
Ag standard (4-0783)	2.5	4	3.8

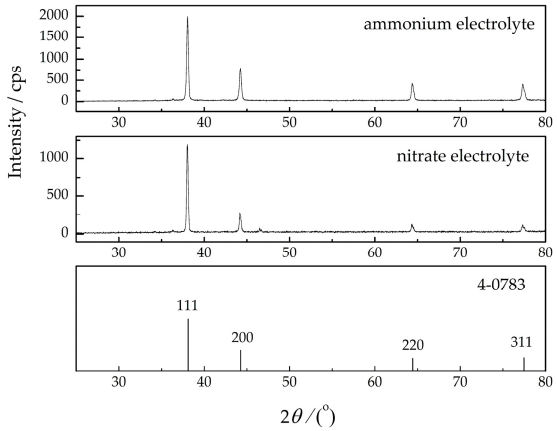

Figure 4. The XRD patterns of the silver powder particles electrodeposited from electrolytes 0.10 M $AgNO_3$ in 2.0 M $NaNO_3$ (the nitrate electrolyte) and 0.10 M $AgNO_3$ in 0.50 M $(NH_4)_2SO_4$ with the addition of NH_3 to dissolve the silver sulfate precipitate (the ammonium electrolyte), as well as the Ag standard (4-0783).

It can be seen from Table 1 that the obtained ratios were approximately twice as large for the particles obtained from the nitrate electrolyte than those characterizing the Ag standard determined by polycrystalline silver with randomly-distributed grains [28]. In this way, non-spherical morphology of silver observed by the SEM technique (Figure 2) was confirmed. On the other hand, the values of intensity ratio for the particles obtained from the ammonium electrolyte were very close to those characterizing the Ag standard. The obtained values were in accordance with results of SEM analysis (Figure 3) that can be explained by the presence of spherical grains in the structure of pine-like dendrites (some of them are shown in circles in Figure 3e).

A more precise analysis of crystallographic structure was obtained by the determination of the "Texture Coefficient", *TC*(*hkl*), and the "relative texture coefficient", *RTC*(*hkl*). These coefficients were calculated using Equations (1)–(3) and the data from the XRD patterns, and the obtained values are given in Table 2. The values of *TC*(*hkl*) greater than 1 [27] and *RTC*(*hkl*) above 25% (four (*hkl*) reflections were analyzed in this investigation) indicate the existence of a preferred orientation of the (*hkl*) reflection compared with the random distribution of grains in the Ag standard. On the basis of the calculated coefficients, it can be concluded that the Ag particles obtained from the nitrate electrolyte possesses the strong (111) preferred orientation, while those obtained from the ammonium electrolyte possesses weak (111) and (200) preferred orientation. However, since the values for the particles produced from the ammonium electrolyte were very close to 1 and 25%, we can also claim that there is a random orientation of Ag crystallites in these particles.

Table 2. Texture calculations for Ag powders obtained by various electrochemical and chemical methods of synthesis (the nitrate electrolyte—NIT, the ammonium electrolyte—AM, reduction with hydrazine—HYD, S—Ag standard).

Plane (*hkl*)	*R* (in %)			R_s (in %)	*TC*			*RTC* (in %)		
	R_{NIT}	R_{AM}	R_{HYD}		TC_{NIT}	TC_{AM}	TC_{HYD}	RTC_{NIT}	RTC_{AM}	RTC_{HYD}
(111)	69.4	54.9	57.2	52.4	1.32	1.05	1.09	41.6	27.2	28.8
(200)	16.3	21.9	18.9	20.9	0.78	1.05	0.90	24.6	27.2	23.8
(220)	7.4	11.9	12.2	13.1	0.56	0.93	0.93	17.7	24.1	24.6
(311)	6.9	11.3	11.7	13.6	0.51	0.83	0.86	16.1	21.5	22.8

3.2. Chemical Synthesis of Ag Powder: Morphological and Crystallographic Analysis

Morphology of the chemically-synthesized Ag particles is presented in Figure 5. It can be seen from Figure 5 that the obtained particles represent agglomerates of approximately spherical grains, with an average size of about 500 nm and less. The XRD pattern of chemically-produced powder together with Ag standard (4-0783) is shown in Figure 6. As expected, Ag crystallites were dominantly oriented in the (111) plane, with the peaks at 2θ values of 38.1°, 44.3°, 64.4°, and 77.5°. At the first sight, it is clear that the obtained XRD pattern is more similar to the one obtained from the ammonium electrolyte than to the one obtained from the nitrate electrolyte. It is confirmed by the analysis of the peak intensities (111)/(200), (111)/(220), and (111)/(311) for this powder, the values of which are also included in Table 1.

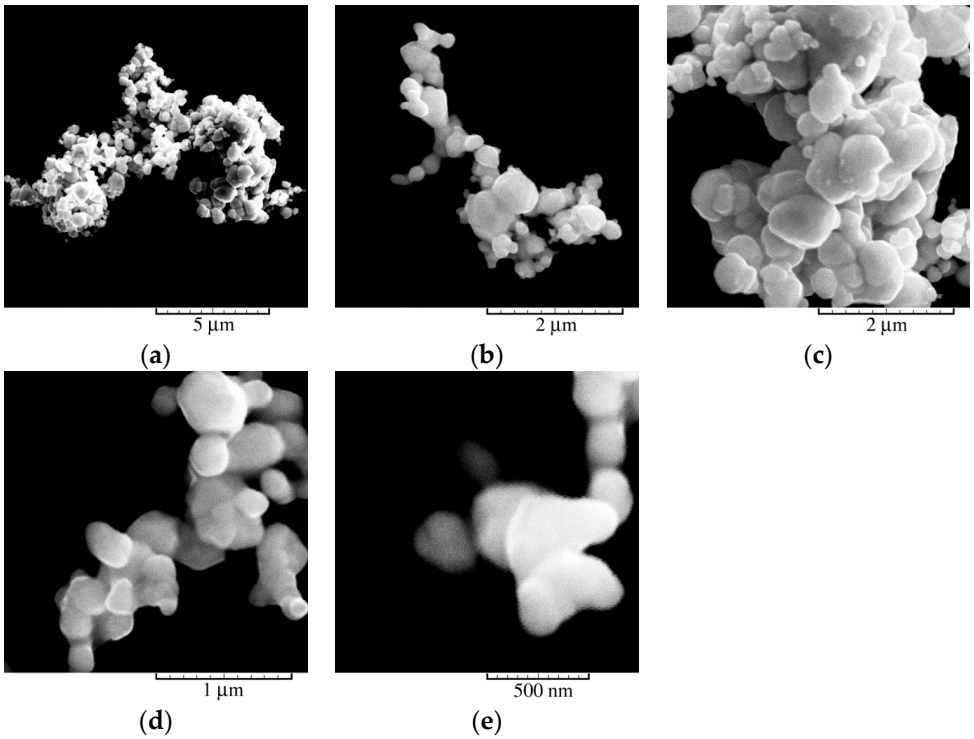

Figure 5. Ag powder particles obtained by chemical reaction with hydrazine as a reducing agent: (**a**,**b**) top view; and (**c**–**e**) the details of the particles shown under (**a**,**b**).

It is understandable because both types of powder particles have similar microstructure consisted of approximately spherical grains with random distribution (Figures 3e and 5d). The similar conclusion can be derived by the analysis of *TC*(*hkl*) and *RTC*(*hkl*) coefficients obtained for this type of the particles (Table 2). Although the obtained values indicated the weak (111) preferred orientation, they are very close to those characterizing the Ag standard confirming a random orientation of the

crystallites in this type of the particles. The specific surface area for the chemically-synthesized powder with hydrazine (SSA_{HYD}) was 0.0298 $m^2 \cdot g^{-1}$, and it was very close to the value obtained for the electrolytically-produced powder from the nitrate electrolyte.

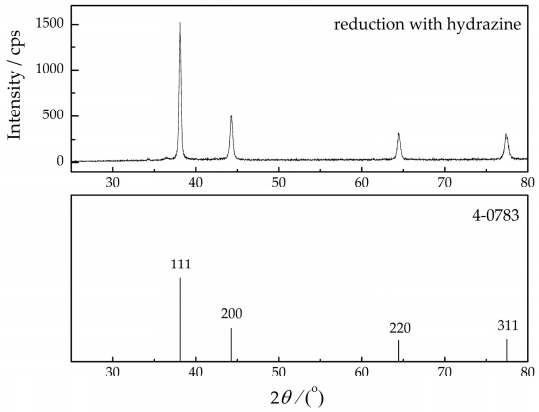

Figure 6. The XRD pattern of the silver powder particles obtained by a chemical reaction with hydrazine as a reducing agent, and Ag standard (4-0783).

4. Discussion

As seen from Figures 2, 3 and 5, the morphology of the powder particles at the macro level was very different. The crystals with well-defined (111) planes as those observed during electrocrystallization of lead [29] can be easily identified among the powder particles obtained from the nitrate electrolyte (Figure 2d,e). The powder particles obtained from this electrolyte showed the strong (111) preferred orientation. On the other hand, the crystals with well-defined crystal planes were not observed among particles electrodeposited from the ammonium electrolyte and those obtained by the reduction with hydrazine. However, although macro morphology of the obtained particles was very different, it can be observed some similarities at the micro level between the powder particles obtained from the ammonium electrolyte and chemically-synthesized particles. Namely, the spherical grains were a characteristic of both types of the particles and the XRD patterns were very close to the Ag standard (Figures 3c–e and 4). In these particles, Ag crystallites were mainly randomly oriented.

The differences in morphologies of electrochemically obtained particles from the nitrate and ammonium electrolytes at the macro level can be explained as follows: The processes of Ag electrodeposition from the nitrate electrolytes belong to the fast electrochemical processes characterized by the high values of the exchange current density ($j_0 \rightarrow \infty$, and $j_0 >> j_L$, where j_0 is the exchange current density and j_L is the limiting diffusion current density), low melting points, and the high overpotentials for hydrogen discharge [30,31]. Due to these characteristics, Ag is situated into the group of the normal metals, together with Pb, Sn, Cd, and Zn. The basic characteristics of electrodeposition of these metals are the diffusion control starting from the small overpotentials and the relatively short plateaus of the limiting diffusion current density [6]. The crystals of regular and irregular shapes and the needle-like dendrites, like those shown in Figure 2, as well as the 2D fern-like dendrites, represent the typical forms of particles obtained by electrodeposition of metals from this group.

On the other hand, ammonium ions construct complexes with Ag(I) ions, lowering the value of the exchange current density for Ag to the value for which $j_0 < j_L$ is valid [6]. For this reason, when electrodeposition was performed from the ammonium electrolyte, Ag is situated, together with Cu and Au, into the group of the intermediate metals. This group of metals is characterized by the lower values of the exchange current density and overpotential for hydrogen evolution reaction than the normal metals. The basic consequences of the decrease of the rate of electrochemical processes, i.e., the j_0 values, are the shift of the plateau of the limiting diffusion current density towards the higher overpotentials, the increase of the plateau of the limiting diffusion current density, and the strong change in the surface

morphology. As result of this, the polarization and morphological characteristics of Ag become similar to those of Cu, which is the typical representative of the group of the intermediate metals. For example, the width of the plateau of the limiting diffusion current density for 0.10 M $CuSO_4$ in 0.50 M H_2SO_4 is between 300 and 750 mV, and it is very comparable with the width of the plateau for Ag from the ammonium electrolyte (250–700 mV). Simultaneously, the shape of the 3D pine-like Ag dendrites (Figure 3) is very similar to Cu dendrites [32].

The Ag dendrites from the ammonium electrolyte were very similar to Ag dendrites obtained in the presence of tungstosilicate [33] and citric [28] acids. The common characteristic of these electrolytes for Ag electrodeposition is their affiliation to the group of complex electrolytes, indicating the strong correlation between the shape of dendritic particles and the type of used electrolyte. Due to the highly-branched structure, the pine-like shape of dendrites show good characteristics determining the behavior of metal powders as a whole [6]. The most important characteristics, denoted as decisive ones, are: the specific surface, the apparent density, the flowability, the particle grain size, and the particle size distribution. This is confirmed by the higher value of SSA for the powder obtained from the ammonium electrolyte than for the one obtained from the nitrate electrolyte.

The effect of the type of electrolyte and, consequently, the rate of the electrochemical process on morphological characteristics of Ag, was larger than in the case of lead, which can be explained by a comparison of the strength of complexes made with Pb and the acetate ions and Ag with the ammonium ions [34]. Namely, Pb makes weaker complexes with the acetate ions than Ag with the ammonium ions, and the strength of this Pb complex was not enough high to transfer Pb from the group of the normal metals into the group of the intermediate metals. The plateau of the limiting diffusion current density was only for about 10 mV wider for the acetate than for the nitrate electrolyte, and slightly shifted to the higher overpotentials at the polarization curve [34]. The 2D needle-like dendrites and irregular crystals predominately formed by Pb electrodeposition from the nitrate electrolytes [6] were very similar to Ag particles formed from the same type of electrolyte. On the other hand, the 2D Pb fern-like dendrites with clearly-defined primary and secondary branches, in accordance with Wranglen's definition of dendrites [35], were formed by electrodeposition from the acetate electrolyte. Hence, the change in the shape of dendrites from the 2D needle-like to the 2D fern-like was observed with use of the complex (acetate) electrolyte for the Pb electrodeposition. This change was weaker than in the case of Ag electrodeposition when the stronger change in the shape of dendrites from the 2D needle-like (the nitrate electrolyte) to the 3D pine-like (the complex (ammonium) electrolyte) was observed.

The strong (111) preferred orientation of electrochemically-produced particles from the nitrate electrolyte can be ascribed to the lower surface energy of the (111) plane in relation to other planes, such as (200), (220), and (311) ones, since the values of surface energy follow the trend $\gamma_{111} < \gamma_{100} < \gamma_{110}$ [36,37]. It means that the rates of electrodeposition for a face centered cubic (FCC) lattice increase in the order of (110) > (100) > (111) [38,39]. The different electrodeposition rate onto different crystal faces will cause a disappearance of fast-growing faces and a survival of slow-growing ones. The origin of Ag crystallites oriented in the (111) plane is of growth centers present in the interior of crystal faces [35,40], and this type of growth centers are denoted as "center type". On the other hand, the origin of Ag crystallites oriented in the (200), (220), and (311) planes is of growth centers present on the edges and corners of growing forms (as "edge and corner type") [35,40]. The current densities responsible for the crystal growth based on growth centers of "edge and corner type" are higher than those responsible for crystal growth based on growth centers of "center type". This means that the current densities are higher at the tips of the growing forms than at their sides. In the growth process, the slow-growing (111) face will survive constructing dendrites and, hence, causing the predominant orientation of Ag crystallites in this plane, as confirmed in Figure 4. On the other hand, it is clear that the (200), (220), and (311) belong to the group of fast-growing faces which the ratio decreases in the growth process. In this way, the larger ratios of Ag crystallites oriented in (200), (220), and (311) planes in the XRD pattern obtained for the particles produced in the ammonium electrolyte in relation

to those obtained from the nitrate electrolyte can be ascribed to the more branched structure and, hence, to the larger number of the tips of the pine-like dendrites caused by the decrease of the rate of electrochemical process.

The shape of chemically-produced Ag particles (agglomerates of spherical or globular grains) obtained with hydrazine was very similar to the particles obtained with formaldehyde as reducing agent [18]. In both cases, Ag particles were formed from complex $[Ag(NH_3)_2]^+$ ions. Simultaneously, bulbous particles of Ag are formed via galvanic displacement deposition onto aluminum surface from the ammonium solution [6,19]. On the other hand, Ag dendritic particles are formed by galvanic displacement deposition on germanium substrate from acidic Ag(I) solution at pH 2 [6,20], or in citric acid solution on an aluminum surface [6,19]. This indicates the strong correlation between the pH solution and the morphology of chemically-produced particles at the macro level.

Finally, the following comparison and discussion can be made. Unlike of agglomerates of spherical grains formed with hydrazine from the ammonium electrolyte, the particles of dendritic shape are formed from the same type of electrolyte via the electrochemical route. Although morphologies of these particles were very different at the macro level, the similarity at the micro level can be established. The both agglomerates of grains and dendrites are consisted of spherical grains. This was accompanied by the similar XRD patterns of the particles obtained by reduction with hydrazine and those obtained by electrolysis from the ammonium electrolyte. These XRD patterns were very similar to Ag standard confirming the existence of spherical morphology of silver at the micro level.

Application of Ag powders is closely associated with the morphology of the particles. For example, the particles in the form of agglomerates consisted of spherical grains like those shown in Figure 5 are widely used in fabrication of conductive pastes for electronic industry [41]. The particles of dendritic shape have very high surface area and, as such, are widely used in catalysis [42], fabrication of sensors [5], as superhydrophobic surface [24], in surface-enhanced Raman scattering (SERS) [24], as well as in surface-enhanced fluorescence (SEF) [24].

5. Conclusions

Morphologies of Ag particles produced by electrolysis from the basic (nitrate) and the complex (ammonium) electrolytes were compared with chemically-synthesized particles using hydrazine as the reducing agent, and correlated with the corresponding crystallographic characteristics. Depending on the method of preparation, various morphologies of Ag particles were observed at the macro level. The mixture of crystals of regular (with clearly-defined crystal planes) and irregular shape and the 2D needle-like dendrites were formed by electrolysis from the nitrate electrolyte. The 3D pine-like dendrites with spherical grains were produced by electrolysis from the ammonium electrolyte and, finally, agglomerates of spherical grains were obtained via the chemical route with hydrazine. In spite of the very different morphologies at the macro level, the similarity at the micro level was observed between the electrolytically-produced powder particles from the ammonium electrolyte and chemically-synthesized powder particles. Namely, the common characteristic of these powder particles was the presence of the spherical grains that were constructed.

The strong (111) preferred orientation was a characteristic of the particles obtained by electrolysis from the nitrate electrolyte. The Ag crystallites were randomly oriented in the particles obtained by the electrolysis from the ammonium electrolyte, as well as in those chemically-synthesized with hydrazine. These XRD patterns were very similar to the Ag standard which is explained by the existence of the spherical morphology in these particles. In this way, correlation between morphologies of powder particles obtained by different methods of synthesis and the corresponding crystallographic characteristics was, for the first time, established at the semi-quantitative level. The specific surface area (SSA) of the powders increased in the row: $SSA_{HYD} < SSA_{NIT} < SSA_{AM}$.

The different morphologies of electrochemically produced powder particles from the nitrate and ammonium electrolytes are ascribed to the decrease of the rate of electrochemical processes caused by the formation of the Ag complex with the ammonium ions. This decrease of the rate of

the electrochemical process achieved a strong effect on the crystallographic characteristics of the formed particles through the larger ratios of Ag crystallites oriented in (200), (220), and (311) planes, i.e., in fast-growing planes, in the Ag particles obtained from the ammonium electrolyte in relation to those obtained from the nitrate electrolyte. For these reasons, the Ag particles obtained from the nitrate electrolyte possessed the strong (111) preferred orientation, while Ag crystallites in the particles obtained from the ammonium electrolyte were randomly oriented.

Acknowledgments: This work was supported by the Ministry of Education, Science, and Technological Development of the Republic of Serbia under the research project: "Electrochemical synthesis and characterization of nanostructured functional materials for application in new technologies" (project no. 172046).

Author Contributions: Ljiljana Avramović performed the formation of silver crystals by an electrolytic procedure; Miroslav M. Pavlović performed the preparation of electrolytically- and chemically-produced silver crystals for XRD and SEM analysis; Vesna M. Maksimović performed the XRD analysis and the discussion of the corresponding data; Marina Vuković performed the SEM characterization of silver particles; Jasmina S. Stevanović performed the chemical synthesis; Mile Bugarin provided reagents and equipment for the electrochemical experiments; and Nebojša D. Nikolić conceived and wrote the paper.

Conflicts of Interest: The authors declare no conflict of interest.

References

1. Antony, L.V.M.; Reddy, R.G. Processes for Production of High-Purity Metal Powders. *JOM* **2003**, *55*, 14–18. [CrossRef]
2. Chaubey, A.K.; Scudino, S.; Khoshkhoo, M.S.; Prashanth, K.G.; Mukhopadhyay, N.K.; Mishra, B.K.; Eckert, J. Synthesis and Characterization of Nanocrystalline Mg-7.4%Al Powders Produced by Mechanical Alloying. *Metals* **2013**, *3*, 58–68. [CrossRef]
3. Calusaru, A. *Electrodeposition of Metal Powders*; Elsevier: New York, NY, USA, 1979; pp. 1–544.
4. Orhan, G.; Hapci, G. Effect of electrolysis parameters on the morphologies of copper powder obtained in a rotating cylinder electrode cell. *Powder Technol.* **2010**, *201*, 57–63. [CrossRef]
5. Amiri, M.; Nouhi, S.; Azizian-Kalandaragh, Y. Facile synthesis of silver nanostructures by using various deposition potential and time: A nonenzymatic sensors for hydrogen peroxide. *Mater. Chem. Phys.* **2015**, *155*, 129–135. [CrossRef]
6. Popov, K.I.; Djokić, S.S.; Nikolić, N.D.; Jović, V.D. *Morphology of Electrochemically and Chemically Deposited Metals*; Springer: New York, NY, USA, 2016; pp. 1–368.
7. Nikolić, N.D.; Branković, G.; Pavlović, M.G. Correlate between morphology of powder particles obtained by the different regimes of electrolysis and the quantity of evolved hydrogen. *Powder Technol.* **2012**, *221*, 271–277.
8. Yao, C.-Z.; Liu, M.; Zhang, P.; He, X.-H.; Li, G.-R.; Zhao, W.-X.; Liu, P.; Tong, Y.-X. Tuning the architectures of lead deposits on metal substrates by electrodeposition. *Electrochim. Acta* **2008**, *54*, 247–253. [CrossRef]
9. Ni, Y.; Zhang, Y.; Hong, J. Hierarchical Pb microstructures: A facile electrochemical synthesis, shape evolution and influencing factors. *CrystEngComm* **2011**, *13*, 934–940. [CrossRef]
10. Cherevko, S.; Xing, X.; Chung, C.-H. Hydrogen template assisted electrodeposition of sub-micrometer wires composing honeycomb-like porous Pb films. *Appl. Surf. Sci.* **2011**, *257*, 8054–8061. [CrossRef]
11. Yang, M. Fern-shaped bismuth dendrites electrodeposited at hydrogen evolution potentials. *J. Mater. Chem.* **2011**, *21*, 3119–3124. [CrossRef]
12. Bengoa, L.N.; Bruno, S.; Lazzarino, H.A.; Seré, P.R.; Egli, W.A. Study of dendritic growth of zinc crystals on the edges of steel sheet. *J. Appl. Electrochem.* **2014**, *44*, 1261–1269. [CrossRef]
13. Wang, J.; Wei, L.; Zhang, L.; Zhang, Y.; Jiang, C. Electrolytic approach towards the controllable synthesis of symmetric, hierarchical, and highly ordered nickel dendritic crystals. *CrystEngComm* **2012**, *14*, 1629–1636. [CrossRef]
14. Lv, Z.-Y.; Li, A.-Q.; Fei, Y.; Li, Z.; Chen, J.-R.; Wang, A.-J.; Feng, J.-J. Facile and controlled electrochemical route to three-dimensional hierarchical dendritic gold nanostructures. *Electrochim. Acta* **2013**, *109*, 136–144. [CrossRef]

15. Ostanina, T.N.; Rudoi, V.M.; Patrushev, A.V.; Darintseva, A.B.; Farlenkov, A.S. Modelling the Dynamic Growth of Copper and Zinc Dendritic Deposits under the Galvanostatic Electrolysis Conditions. *J. Electroanal. Chem.* **2015**, *750*, 9–18. [CrossRef]
16. Jović, V.D.; Jović, B.M.; Maksimović, V.M.; Pavlović, M.G. Electrodeposition and morphology of Ni, Co and Ni–Co alloy powders: Part II. Ammonium chloride supporting electrolyte. *Electrochim. Acta* **2007**, *52*, 4254–4263.
17. Nikolić, N.D.; Pavlović, Lj.J.; Pavlović, M.G.; Popov, K.I. Morphologies of electrochemically formed copper powder particles and their dependence on the quantity of evolved hydrogen. *Powder Technol.* **2008**, *185*, 195–201.
18. Djokić, S.S. Production of Metallic Powders from Aqueous Solutions without an External Current Source. In *Electrochemical Production of Metal Powders, Series: Modern Aspects of Electrochemistry*; Djokić, S.S., Ed.; Springer: New York, NY, USA, 2012; Volume 54, pp. 369–398.
19. Djokić, S.S.; Djokić, N.S. Electroless deposition of metallic powders. *J. Electrochem. Soc.* **2011**, *158*, D204–D209.
20. Djokić, S.S.; Djokić, N.S.; Guthy, C.; Thundat, T. Deposition of copper, silver and gold from aqueous solutions onto germanium substrates via galvanic displacement. *Electrochim. Acta* **2013**, *109*, 475–481.
21. Yun, H.D.; Seo, D.M.; Lee, M.Y.; Kwon, S.Y.; Park, L.S. Effective Synthesis and Recovery of Silver Nanowires Prepared by Tapered Continuous Flow Reactor for Flexible and Transparent Conducting Electrode. *Metals* **2016**, *6*, 14. [CrossRef]
22. Maksimović, V.M.; Pavlović, M.G.; Pavlović, Lj.J.; Tomić, M.V.; Jović, V.D. Morphology and growth of electrodeposited silver powder particles. *Hydrometallurgy* **2007**, *86*, 22–26.
23. Popov, K.I.; Živković, P.M.; Nikolić, N.D. Formation of Disperse Silver Deposits by the Electrodeposition Processes at High Overpotentials. *Int. J. Electrochem. Sci.* **2012**, *7*, 686–696.
24. Fu, L.; Tamanna, T.; Hu, W.-J.; Yu, A. Chemical preparation and applications of silver dendrites. *Chem. Pap.* **2014**, *68*, 1283–1297. [CrossRef]
25. Jiang, Z.; Lin, Y.; Xie, Z. Structural investigations and growth mechanism of well-defined Ag dendrites prepared by conventional redox displacement. *Mater. Chem. Phys.* **2012**, *134*, 762–767. [CrossRef]
26. Giannini, C.; Ladisa, M.; Altamura, D.; Siliqi, D.; Sibillano, T.; De Caro, L. X-ray Diffraction: A Powerful Technique for the Multiple-Length-Scale Structural Analysis of Nanomaterials. *Crystals* **2016**, *6*, 87. [CrossRef]
27. Berube, L.P.; Esperance, G.L. A Quantitative Method of Determining of the Degree of Texture of Zinc Electrodeposits. *J. Electrochem. Soc.* **1989**, *136*, 2314–2315. [CrossRef]
28. Mandke, M.V.; Han, S.-H.; Pathan, H.M. Growth of silver dendritic nanostructures via electrochemical route. *CrystEngComm* **2012**, *14*, 86–89. [CrossRef]
29. Nikolić, N.D.; Ivanović, E.R.; Branković, G.; Lačnjevac, U.Č.; Stevanović, S.I.; Stevanović, J.S.; Pavlović, M.G. Electrochemical and crystallographic aspects of lead granular growth. *Metall. Mater. Trans. B* **2015**, *46*, 1760–1774.
30. Winand, R. Electrodeposition of metals and alloys—New results and perspectives. *Electrochim. Acta* **1994**, *39*, 1091–1105. [CrossRef]
31. Kozlov, V.M.; Peraldo Bicelli, L. Influence of the nature of metals on the formation of the deposit's polycrystalline structure during electrocrystallization. *J. Cryst. Growth* **1999**, *203*, 255–260. [CrossRef]
32. Nikolić, N.D.; Popov, K.I.; Pavlović, L.J.; Pavlović, M.G. The effect of hydrogen codeposition on the morphology of copper electrodeposits. I. The concept of effective overpotential. *J. Electroanal. Chem.* **2006**, *588*, 88–98.
33. Han, J.; Liu, J. Electrodeposition of Crystalline Dendritic Silver in 12-Tungstosilicate Acid System. *J. Nanoeng. Nanomanuf.* **2012**, *2*, 171–174. [CrossRef]
34. Nikolić, N.D.; Vaštag, D.D.; Živković, P.M.; Jokić, B.; Branković, G. Influence of the complex formation on the morphology of lead powder particles produced by the electrodeposition processes. *Adv. Powder Technol.* **2013**, *24*, 674–682.
35. Wranglen, G. Dendrites and growth layers in the electrocrystallization of metals. *Electrochim. Acta* **1960**, *2*, 130–146. [CrossRef]
36. Sivasubramanian, R.; Sangaranarayanan, M.V. Electrodeposition of silver nanostructures: From polygons to dendrites. *CrystEngComm* **2013**, *15*, 2052–2056. [CrossRef]
37. Xia, Y.; Xiong, Y. Lim, B; Skrabalak, S.E. Shape-Controlled Synthesis of Metal Nanocrystals: Simple Chemistry Meets Complex Physics? *Angew. Chem. Int. Ed.* **2009**, *48*, 60–103. [CrossRef] [PubMed]

38. Bockris, J.O.; Reddy, A.K.N.; Gamboa-Aldeco, M. *Modern Electrochemistry 2A, Fundamentals of Electrodics*; Kluwer Academic/Plenum Publishers: New York, NY, USA, 2000; p. 1333.
39. Nikolić, N.D.; Maksimović, V.M.; Branković, G.; Živković, P.M.; Pavlović, M.G. Influence of the type of electrolyte on morphological and crystallographic characteristics of lead powder particles. *J. Serbian Chem. Soc.* **2013**, *78*, 1387–1395.
40. Nikolić, N.D.; Maksimović, V.M.; Branković, G. Morphological and crystallographic characteristics of electrodeposited lead from the concentrated electrolyte. *RSC Adv.* **2013**, *3*, 7466–7471.
41. Moudir, N.; Boukennous, Y.; Moulaï-Mostefa, N.; Bozetine, I.; Maoudj, M.; Kamel, N.; Kamel, Z.; Moudir, D. Preparation of silver powder used for solar cell paste by reduction process. *Energy Procedia* **2013**, *36*, 1184–1191. [CrossRef]
42. Sivasubramanian, R.; Sangaranarayanan, M.V. A facile formation of silver dendrites on indium tin oxide surfaces using electrodeposition and amperometric sensing of hydrazine. *Sens. Actuators B* **2015**, *213*, 92–101. [CrossRef]